RPE | Radiation Physics & Engineering
An International Peer-Reviewed Journal
Published by K.N. Toosi University of Technology
http://rpe.kntu.ac.ir
Research Article

Radiation Physics and Engineering 2021; 2(2):13–19
https://doi.org/10.22034/rpe.2021.295907.1032

# Scintillation properties of CsI(Tl) co-doped with $Tm^{2+}$

Sajjad Shahmaleki, Faezeh Rahmani*
*Department of Physics, K.N. Toosi University of Technology, P.O. Box 15875-4416, Tehran, Iran*

## HIGHLIGHTS

- Investigation on the scintillation characteristics of CsI(Tl) codopant with Tm.
- Less afterglow relates to 0.05 mol% of Tm regardless to Tl concentrations.
- CsI(Tl,Tm) can be a good choice for high frequency X-ray, gamma spectroscopy and imaging.
- A new method was proposed based on the variation of integration time for evaluating the afterglow.

## ABSTRACT

In this research, the Tm content as codopant in CsI(Tl) was optimized for reducing the afterglow. As an experimental reference, CsI(Tl) and CsI(Tl-0.05%Eu) single crystals were grown by Bridgman method. The grown crystals were characterized through photoluminescence analysis, and the measurements of charge collection time, energy resolution, photon light yield as well as the amount of afterglow were performed. It was observed that the change in codopant shifted the emission curve of $Tl^+$. For CsI(Tl) codoped with Tm in the range of 0.02 to 0.1 mol%, the afterglow of 0.05 mol% Tm reduced in comparison with Tm-free CsI(Tl). The results showed that the Tm codopant resulted in a decrease of 32 to 42% in afterglow depending on the Tl concentration. The addition of various contents of Tm also decreased the light yield up to 23%, and the resolution by about 2 to 33%. The light yield exhibited insignificant changes, whilst the measured energy resolution was about 8.8% at 662 keV. Overall, the improvement in the afterglow, as well as the insignificant reduction in both the energy resolution and light yield of CsI(Tl-Tm), may motivate some researchers to consider it as a good candidate for fast spectroscopy and high-frequency imaging applications.

## KEYWORDS

CsI(Tl)
Codopant
Afterglow
Light yield
Gamma-ray spectroscopy

## HISTORY

Received: 19 July 2021
Revised: 14 September 2021
Accepted: 15 September 2021
Published: Spring 2021

## 1 Introduction

CsI(Tl) scintillator was discovered in 1951 (Van Sciver and Hofstadter, 1951), representing 66,000 photons/MeV light yield, about 1000 ns decay time, and an emission band at 550 nm with perfect optical coupling with photomultiplier tube (PMT) glass window (Nikl, 2006), the effective atomic number of 54, the density of 4.53 $g.cm^{-3}$, and the capability to be grown as a single crystal. CsI(Tl) is widely used in radiation applications such as gamma- and X-ray spectroscopy and imaging (Wu et al., 2014b; Rodnyi, 2020; Knoll and Glein, 1989). However, there is a limit in high-frequency imaging and computerized tomography due to the long afterglow of CsI(Tl) (Siewerdsen and Jaffray, 1999; Thacker et al., 2009). A very small amount of appropriate dopants (*i.e.* in order of ppm) may modify the scintillation characteristics, so various methods and techniques have been studied to improve the scintillation characteristics of CsI(Tl) over the last two decades (Brecher et al., 2006; Bartram et al., 2006; Totsuka et al., 2012; Wu et al., 2014a; Nagarkar et al., 2008; Kappers et al., 2010; Wu et al., 2014c; Ovechkina et al., 2007). These studies show that the afterglow is efficiently decreased by using some codopants such as $Yb^{2+}$, $Sm^{3+}$, $Eu^{2+}$, and $Bi^{2+}$. For example, $Sm^{2+}$ rare-earth ions may reduce the afterglow by about 0.1% after 1 s by X-ray irradiation (Nagarkar et al., 2008; Kappers et al., 2010), and to 0.1% using $Bi^{3+}$ codopant after 10 ms under low-energy X-ray (Totsuka et al., 2012). Besides afterglow improvement, the $Eu^{2+}$, $Bi^{3+}$, and $Sm^{2+}$ ions may have undesirable effects on other scintillation characteristics. However, the studies show that $Yb^{2+}$ enhances all scintillation characteristics (Wu et al., 2014c). In general, using lanthanide codopants can effectively improve most scintillation characteristics of CsI(Tl).

This study aims to explore the scintillation proper-

*Corresponding author: frahmani@kntu.ac.ir

ties of CsI(Tl) codoped with Tm, which has not been reported in literature so far. For better evaluation and comparison of experimental data, CsI(Tl) single crystals with/without Eu have also been grown using the vertical Bridgman method. The grown crystals have been characterized through photoluminescence analysis, and the measurements of charge collection time, energy resolution, photon light yield as well as the amount of afterglow. In addition, a novel gamma-ray spectroscopy method has been proposed to evaluate both the scintillator quality and micro-second scale decay-time measurements.

## 2 Materials and Methods

### 2.1 Crystal growth

Single crystals were grown by the vertical Bridgman method with and without dopants. The starting concentrations were in the range of 0.2 mol% for Tl (as the main dopant), 0.05 mol% for Eu (as a reference sample), and 0.02 to 0.1 mol% for Tm (as a codopant). High-purity raw materials from Merck and Sigma-Aldrich (www.Merck.com, https://www.sigmaaldrich.com) were loaded in cylindrical quartz ampoules (with a conical tip and slope of 45°) before being heated in the vacuum for moisture removal. To ensure homogenized melting of the CsI, the ampoules were kept at 700 °C for 5 hours. Next, they were pulled up within an optimal temperature with a velocity of 1 mm.h$^{-1}$.

To obtain a uniform distribution of dopants, the grown crystals were heated at 500 °C for 24 hours. Single crystals were right cylinders (with an initial dimension of 20 mm in diameter and thickness) with a conical tip. All crystals were transparent and colorless. Then all samples were polished with a finished thickness of 10 mm (with a final dimension of 20 mm in diameter and 10 mm in thickness). To provide the diffuse reflection at the scintillator surface, Teflon tape was used for wrapping these specimens before measuring the luminescence spectrum, decay-time value, pulse-height spectrum, and energy resolution.

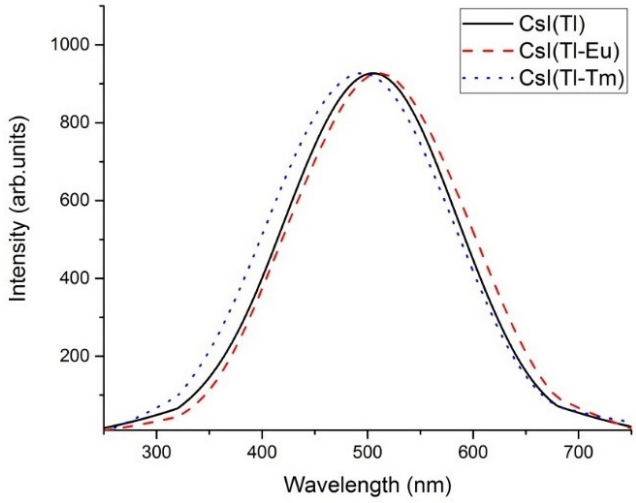


**Figure 1:** Emission spectra of CsI(Tl) and co-doped samples with 0.05 mol% Tm2+ and 0.05mol% $Eu^{2+}$ contents under continuous UV (236 nm) irradiations.

### 2.2 Measurement of optical and scintillation properties

The *photoluminescence spectra* were measured using the LS55-Perkin Elmer system within the wavelength range of 200 to 800 nm at room temperature. The spectra of photoluminescence emission and excitation of CsI crystals are presented in Fig. 1.

Photonis XP2020 photomultiplier tube (with a bialkali photocathode, 12-stage dynode chain with 1.7 ns rise time) was used for charge-collection time measurements [www.Photonis.com], whilst silicon oil was used for better optical coupling of scintillator crystal to PMT glass window and Teflon tape was wrapped around the scintillator surface for better light-collection efficiency. Output pulses of the PMT anode were fed into a 500 MHz/8-bit digitizer. The pulses were recorded and analyzed by MATLAB software (www.Matlab.com) (Ghorbani et al., 2019), and the average pulse was calculated based on averaging 4 ns step point-by-point. The duration of each measurement (containing 10,000 pulses) was about 10 minutes. Figure 2 shows a schematic view of the experimental setup for recording the anode pulses using a 1 $\mu$Ci Cs-137 gamma-ray source.

For *studying the afterglow characteristics*, a 2-inch Photonis XP2020 PMT operated at -1800 V, an Ortec 672 amplifier, a Canberra 2005 fast preamplifier, and a multichannel analyzer (MCA) were used. Figure 3 shows a schematic view of the experimental setup for the measurement of afterglow.

The crystals were exposed to a point Cs-137 gamma source at room temperature for 300 s before the integration time was changed by different integration times (*i.e.* shaping times) at a gain of 300. The positions of the photopeak in pulse-height spectra were finally recorded as a function of integration time.

The light yield of the samples was also studied as follows. First, the CsI(Tl) samples were calibrated based on the position of the full energy peak of 662 keV Cs-137 gamma-rays. Then, the CsI(Tl-Eu) and CsI(Tl-Tm) samples were calibrated with respect to the calibrated CsI(Tl) sample. For light yield measurements, the samples were coupled to an XP2020 PMT and exposed to a collimated beam of 662 keV Cs-137 gamma-rays. It should be noted that a Gaussian fit to the data was used for the determination of photopeak positions.

It should be noted that optical coupling, polish quality and earth magnetic field are important parameters that are the same in all experiments.

## 3 Results and discussion

**Photoluminescence measurement**: The presence of codopants will be more evident when the excitation is performed by 236 nm UV irradiation, as shown in the emission spectra of Fig. 1.

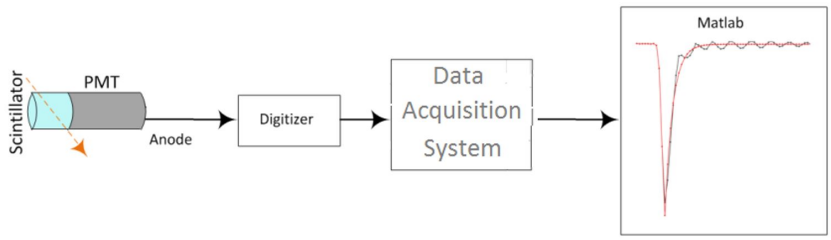


**Figure 2:** Schematic view of the experimental setup for the measurement of charge collection time.

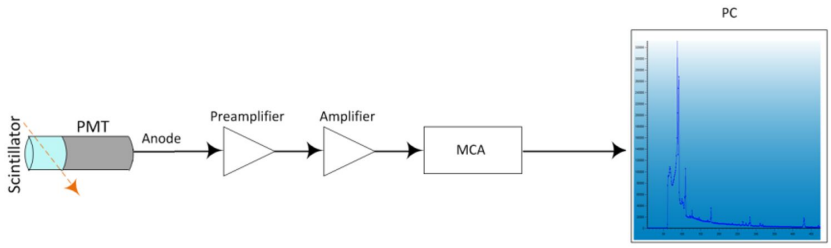


**Figure 3:** Schematic view of the experimental setup for afterglow and decay time measurements.

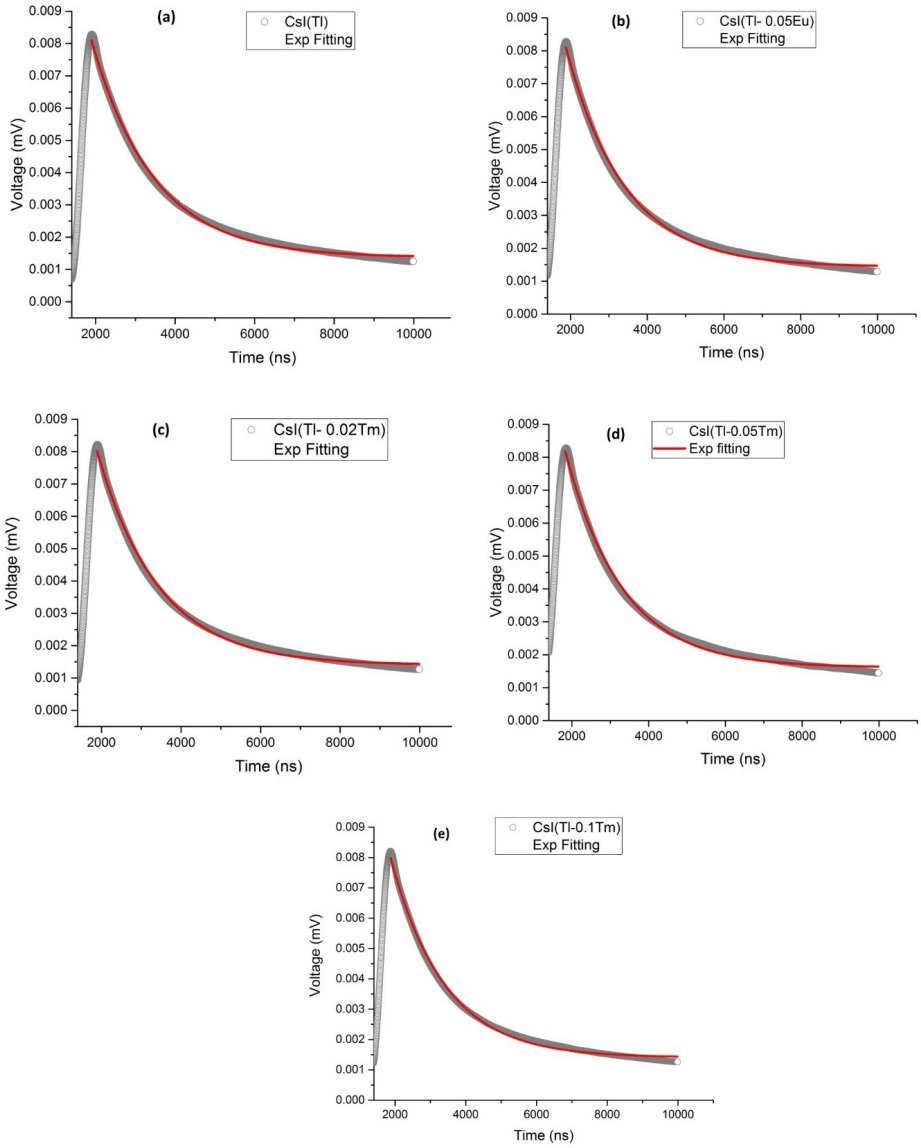


**Figure 4:** The average anode pulses of single crystals: (a) CsI(Tl), (b) CsI(Tl-0.05), (c) CsI(Tl-0.02Tm), (d) CsI(Tl-0.05Tm), (e) CsI(Tl-0.1Tm).

**Table 1:** Decay time components of scintillators measured with averaged anode pulse.

| Sample | CsI (Tl) | CsI (Tl-0.05Eu) | CsI (Tl-0.02Tm) | CsI (Tl-0.05Tm) | CsI (Tl-0.1Tm) |
|---|---|---|---|---|---|
| Charge collection time (ns) | 1561 | 1522 | 1540 | 1467 | 1513 |

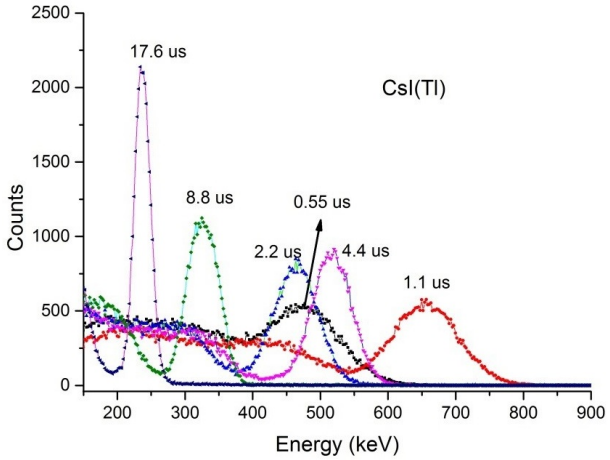


**Figure 5:** Pulse-height spectra labeled with integration times for CsI(Tl) exposed by Cs-137 gamma-rays.

A small change in codopant contents (0.05 mol% Tm/Eu) shifts the peak wavelengths to 490 and 520 nm, which may be related to the emission band of $Tm^{2+}$ and $Eu^{2+}$ codopants. These results are in good agreement with the previously published data (Brecher et al., 2006).

$Tl^{+}$ ions absorb most excitation photons of 236 nm UV irradiation which is the reason for the small displacement in the $Tl^{+}$ position in emission spectra. The corresponding photon counts of $Tm^{2+}$ and $Eu^{2+}$ codoped samples differ from that of Cs(Tl) as much as 10% and 6%, respectively. The maximum emission wavelength of $Tl^{+}$ is observed at 510 nm.

**Charge collection time measurement**: Figure 2 shows a schematic view of the experimental setup employed to record anode pulses. The average anode pulses (i.e., the inverted positive average pulse-shape) of the samples (with Teflon covering) exposed to Cs-137 gamma-rays are shown in Fig. 4. A single exponential curve (denoted by EXP) has been fitted to data of the decay regions of the charge collection time profiles of CsI(Tl), CsI(Tl-0.05Eu), and CsI(Tl-Tm) single crystals.

Table 1 summarizes the charge collection time of CsI(Tl-0.05Eu) and CsI(Tl-Tm) single crystals. These time constants of scintillation curves are much faster than the time component of CsI(Tl), which means that the $Tm^{2+}$ or $Eu^{2+}$ codopants can effectively suppress the slow components. The relative errors of charge collection time measurements were less than 0.2%.

**Afterglow and decay time measurements**: Figure 5 illustrates the pulse-height spectra and the integration times for the CsI(Tl) sample exposed to Cs-137 gamma-rays. The integration time depends on the charge collection time which is itself a function of the time constant of output circuit.

As shown in Fig. 5, the photopeak position is considerably shifted towards the higher channels when the integration time (*i.e.* shaping time) of the amplifier is decreased. The same behavior is seen up to the maximum integration time, where the photopeak moves to the lower channels. This can be understood by analyzing the electronic response of the amplifier and the time response of the detector.

At relatively short times, the amplifier prevents the maximum output signals from reaching the actual values. However, the maximum amplitude of the output signal approaches its actual value by increasing time, which increases photopeak positions.

Alternatively, when the time reaches beyond the maximum integration time, the pulse pile-up may also occur at the amplifier output, and hence, the MCA fails in measuring the maximum amplitude of its output signal. Therefore, the amplitude of the measured signal would be lower than the position of photopeak. Since the light collection efficiency is different in various scintillators, the maximum integration time would be different, as well.

The pulse-height spectrum corresponding to the integration time in the CsI(Tl) at 662 keV is shown in Fig. 5. As shown, by increasing the integration time from 0.55 to 1.1 $\mu$s, the corresponding channel of photopeak position is increased with the maximum value of about 1.1 $\mu$s. By increasing the integration time from 1.1 to 2.2 $\mu$s, the photopeak channel moves to smaller values, whilst by increasing the integration time from 2.2 to 4.2 $\mu$s, the photopeak channel is increased again. At an integration time of 4.2 $\mu$s, this trend continues to reach another maximum position of photopeak. As seen, increasing the integration time from 4.2 to 17.6 $\mu$s leads to an increase in photopeak position.

The scintillation decay time of CsI(Tl) detector has two components of 1.1 and 4.4 $\mu$s (https://www.crystals.saint-gobain.com) (Wu et al., 2015).

As seen in the above-mentioned results, the number of generated photons and the corresponding photopeak positions of 1.1 and 4.4 $\mu$s are higher than other decay times. This behavior has also been observed for CsI(Tl-Tm) and CsI(Tl-0.05Eu). The photopeak position versus integration time using Cs-137 source is shown in Fig. 6.

Since the Tl sub-level structure in CsI(Tl-0.05Eu) and CsI(Tl-Tm) crystal lattice is similar to CsI(Tl) scintillator, they have identical fast and slow scintillation decay times. As shown in Fig. 6, these two peaks are corresponding to 1.1 $\mu$s (spectrum A in Fig. 6) and 4.4 s (spectrum B in Fig. 6), respectively.

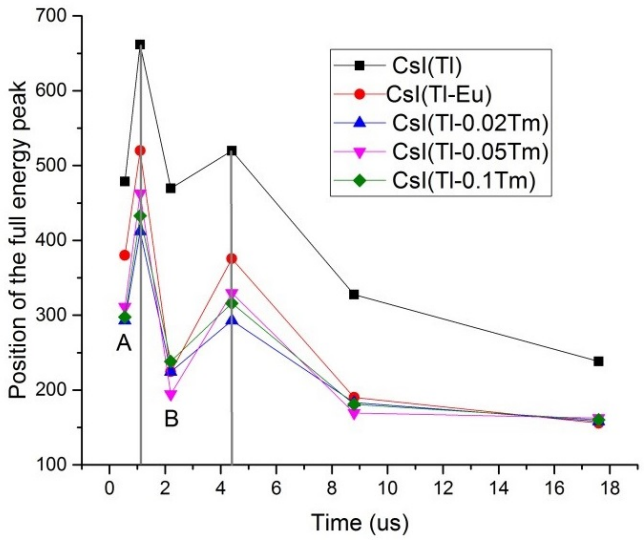


**Figure 6:** The photopeak position versus integration time of the anode signal measured for CsI(Tl), CsI(Tl-Tm ), and CsI(Tl-0.05Eu) samples.

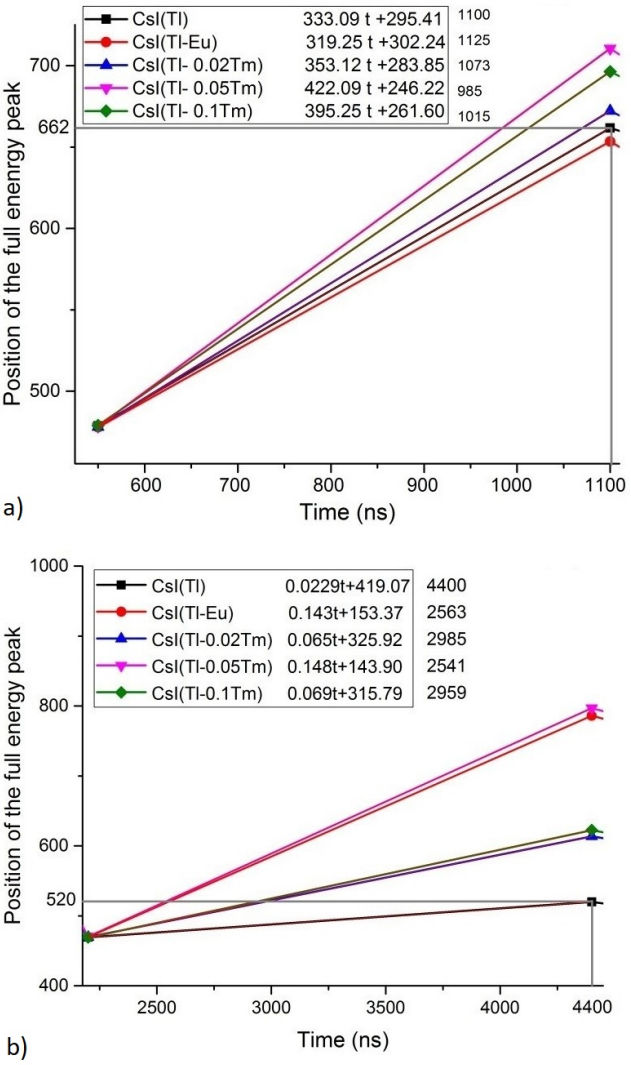


**Figure 7:** The photopeak position of CsI(Tl) sample in (a) region A, (b) region B.

Having employed this new method, the ability to measure both fast and slow components of decay time has been demonstrated. In this method, the fast and slow scintillation decay times of the samples should be compared with CsI(Tl). In order to determine the two decay times for the CsI(Tl) (with Eu/Tm and codopant free), a comparison is undertaken on A and B regions (marked in Fig. 6). The slopes of curves are plotted and distinguished for the samples in Figs. 7-a and 7-b. The decay times can be calculated according to the photopeak positions.

Using the proposed method, the slow and fast decay times were determined as 4.4 and 1.1 s, respectively. These measurements have been performed for other samples with different $Tm^{2+}$ and $Eu^{2+}$ (0.05mol%) codopant concentrations, as well as for CsI(Tl) grown in this work as a control sample. By comparing the decay times in each case, the fast and slow decay times can be determined. The fast and slow decay times of the CsI(Tl-Eu) sample are 1125 and 2563 ns, respectively. The decay times for the samples with 0.02, 0.05, and 0.1 mol% of Tm codopant are listed in Table 2. The relative errors of anode pulse measurements were less than 1%.

Since the slow scintillation decay time is directly proportional to the afterglow of the samples, CsI(Tl-Eu) and CsI(Tl-Tm) with shorter slow decay times exhibit smaller afterglow relative to CsI(Tl). The afterglow component of CsI(Tl-Eu) crystal is much shorter than the decay component of CsI(Tl) (Brecher et al., 2006).

The results of CsI(Tl) codoped with Eu2+ show slower afterglow than CsI(Tl). By adding Tm to CsI(Tl) crystal, the releasing time of the electrons trapped in the lattice becomes shorter, which results in shorter afterglow in comparison with the CsI(Tl) sample. The slow scintillation decay time of CsI(Tl-0.05 mol% Tm), which is about 2541 ns, is slightly shorter than CsI(Tl) codoped with $Tm^{2+}$. This new proposed method can be used for simple assessing the quality of the grown crystals.

**Photon light yield measurement**: The pulse-height spectra of CsI(Tl) crystals with different concentrations of Tm and Eu exposed by Cs-137 (662 keV) are shown in Fig. 8. According to the proportional change in light yield corresponding to different concentrations of codopants, a displacement in photopeak positions can be predicted. Under these conditions, if the light yield of the CsI(Tl) is considered about 100% relative to its channel number, the light yield of the CsI(Tl-0.05Eu) will be about 92%, and, the light yield of the 0.02, 0.05, and 0.1 mol% of Tm will be about 77, 99, and 82%, respectively. Based on these results, the light yield of CsI(Tl-0.05 mol% Tm) (about 99%) is slightly higher than the samples with Tm codopants.

Energy resolution measurement: The energy resolution of CsI(Tl) at 662 keV is about 8.6% (Fig. 8 and Table 2). As far as the Tl content is concerned, this value is comparable with the energy resolution of 10.6% reported in Ref [9]. The energy resolutions measured for 0.02, 0.05, and 0.1 mol% Tm codoped samples are 11, 8.8, and 11.47%, respectively (Table 3). The energy resolution of the CsI(Tl-0.05Tm) sample is about 8.8%, which is similar to CsI(Tl) crystals codoped with different concentrations of Tm. According to the experimental results, the energy resolution

**Table 2:** Decay time constants of scintillator samples measured according to the photopeak position and based on the integration time of the anode signal.

| Sample | Fast decay time constant (ns) | Slow decay time constant (ns) |
|---|---|---|
| CsI(Tl) | 1100 | 4400 |
| CsI(Tl-0.05Eu) | 1125 | 2563 |
| CsI(Tl-0.02Tm) | 1073 | 2985 |
| CsI(Tl-0.05Tm) | 985 | 2541 |
| CsI(Tl-0.1Tm) | 1015 | 2959 |

**Table 3:** Scintillation properties of the grown crystals.

| Sample | Energy resolution 662 keV (%) | Photopeak position (keV) | Light yield of CsI(Tl) % |
|---|---|---|---|
| CsI(Tl) | 8.6 | 662 | 100 |
| CsI(Tl-0.05Eu) | 10.3 | 610 | 92 |
| CsI(Tl-0.02Tm) | 11.47 | 516 | 77 |
| CsI(Tl-0.05Tm) | 8.8 | 655 | 99 |
| CsI(Tl-0.1Tm) | 11.0 | 547 | 82 |

of CsI(Tl-0.05Eu) is about 10.3% at 662 keV, which is in agreement withpublished data (Bartram et al., 2006).

It should be noted that energy resolution and the photon light yield of samples with Tm codopant (*i.e.* the decrease in light yield of about 1 to 23% and in energy resolution of about 2-33%) are relatively poorer than that of CsI(Tl).

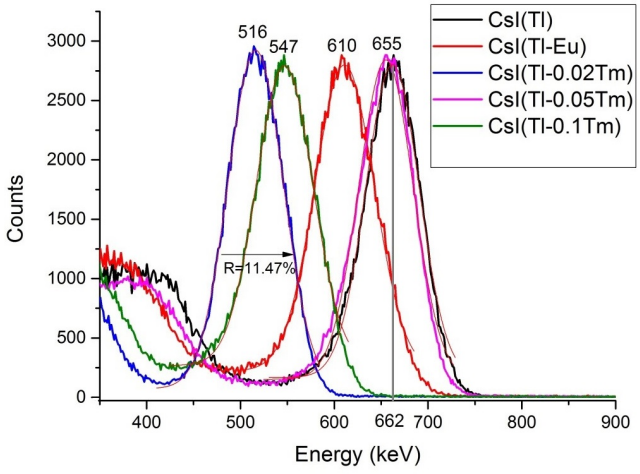


**Figure 8:** Spectra of CsI(Tl) single crystals with different Tm2+contents exposed to Cs-137 source.

## 4 Conclusion

In this research, the scintillation characteristics of CsI(Tl) codopant with Tm, as well as with Eu as a control sample, were studied. A comparative study on the scintillation properties was performed among Tm and Eu codoped CsI(Tl) single crystals grown by the Bridgman method. The light yield, energy resolution, and afterglow show better results in comparison with Tm-free CsI(Tl) (Tables 2 and 3).

Also, a simple and new method based on the variation of integration time has been proposed for the afterglow evaluation of scintillators. Using the proposed method for decay time measurement, the slow decay time, which is directly proportional to the afterglow of the samples, indicates a shorter slow decay time. Therefore, the afterglow has been suppressed in CsI(Tl-Tm) samples relative to other samples. These results were also examined for CsI(Tl-0.05Eu) sample as reported in the literature. The uncertainty of measurements was less than 1%. By introducing Tm codopant into CsI(Tl) lattice, the releasing time of electrons trapped in the lattice becomes shorter, which leads to a shorter afterglow in comparison with CsI(Tl) sample. The amount of afterglow was lowest in 0.05 mol% of Tm regardless of Tl concentrations. It is worthwhile mentioning that this method can be used for evaluating the afterglow in the order of microseconds. Based on the above results, CsI(Tl) codoped with Tm can be a good candidate for high-frequency X-ray and gamma spectroscopy as well as in imaging applications.

## References

Bartram, R., Kappers, L., Hamilton, D., et al. (2006). Suppression of afterglow in CsI: Tl by codoping with Eu2+II: Theoretical model. *Nuclear Instruments and Methods in Physics Research Section A: Accelerators, Spectrometers, Detectors and Associated Equipment*, 558(2):458–467.

Brecher, C., Lempicki, A., Miller, S., et al. (2006). Suppression of afterglow in CsI: Tl by codoping with $Eu^{2+}$I: Experimental. *Nuclear Instruments and Methods in Physics Research Section A: Accelerators, Spectrometers, Detectors and Associated Equipment*, 558(2):450–457.

Ghorbani, P., Sardari, D., Azimirad, R., et al. (2019). Experimental study of a large plastic scintillator response with different reflective coverings based on digital pulse processing method. *Journal of Radioanalytical and Nuclear Chemistry*, 321(2):481–488.

Kappers, L., Bartram, R., Hamilton, D., et al. (2010). A tunneling model for afterglow suppression in CsI: Tl, Sm scintillation materials. *Radiation measurements*, 45(3-6):426–428.

Knoll, G. F. and Glein, F. (1989). Radiation detection and measurement, Wiley. *New York*.

Nagarkar, V., Brecher, C., Ovechkina, E., et al. (2008). Scintillation Properties of CsI: Tl Crystals Codoped With $Sm^{2+}$. *IEEE Transactions on Nuclear Science*, 55(3):1270–1274.

Nikl, M. (2006). Scintillation detectors for x-rays. *Measurement Science and Technology*, 17(4):R37.

Ovechkina, E., Gaysinskiy, V., Miller, S., et al. (2007). Multiple doping of CsI: Tl crystals and its effect on afterglow. *Radiation measurements*, 42(4-5):541–544.

Rodnyi, P. A. (2020). *Physical processes in inorganic scintillators*. CRC press.

Siewerdsen, J. and Jaffray, D. (1999). A ghost story: Spatio-temporal response characteristics of an indirect-detection flat-panel imager. *Medical physics*, 26(8):1624–1641.

Thacker, S., Singh, B., Gaysinskiy, V., et al. (2009). Low-afterglow CsI: Tl microcolumnar films for small animal high-speed microCT. *Nuclear Instruments and Methods in Physics Research Section A: Accelerators, Spectrometers, Detectors and Associated Equipment*, 604(1-2):89–92.

Totsuka, D., Yanagida, T., Fujimoto, Y., et al. (2012). Afterglow suppression by codoping with Bi in CsI: Tl crystal scintillator. *Applied Physics Express*, 5(5):052601.

Van Sciver, W. and Hofstadter, R. (1951). Scintillations in Thallium-Activated CaI2 and CsI. *Physical Review*, 84(5):1062.

Wu, Y., Ren, G., Meng, F., et al. (2014a). Ultralow-concentration Sm codoping in CsI: Tl scintillator: A case of little things can make a big difference. *Optical Materials*, 38:297–300.

Wu, Y., Ren, G., Meng, F., et al. (2015). Scintillation characteristics of indium doped cesium iodide single crystal. *IEEE Transactions on Nuclear Science*, 62(2):571–576.

Wu, Y., Ren, G., Nikl, M., et al. (2014b). CsI: $Tl^{+}$, $Yb^{2+}$: ultra-high light yield scintillator with reduced afterglow. *CrystEngComm*, 16(16):3312–3317.

Wu, Y., Ren, G., Nikl, M., et al. (2014c). CsI: Tl+, Yb2+: ultra-high light yield scintillator with reduced afterglow. *CrystEngComm*, 16(16):3312–3317.